Estimating the actual dose delivered by intravascular coronary brachytherapy using geometrically correct 3-D modeling

Andreas Wahle,[a] John J. Lopez,[b,d] Edward C. Pennington,[c] Sanford L. Meeks,[c] Kathleen C. Braddy,[b] James M. Fox,[b] Theresa M. H. Brennan,[b] John M. Buatti,[c] James D. Rossen,[b] and Milan Sonka[a]

The University of Iowa, [a]Department of Electrical and Computer Engineering, [b]Department of Internal Medicine, and [c]Department of Radiation Oncology, Iowa City, IA 52242, USA

[d]The University of Chicago, Department of Medicine, Chicago, IL 60637, USA

ABSTRACT

Intravascular brachytherapy has shown to reduce re-occurrence of in-stent restenosis in coronary arteries. For beta radiation, application time is determined from source activity and the angiographically estimated vessel diameter. Conventionally used dosing models assume a straight vessel with the catheter centered and a constant-diameter circular cross section. Aim of this study was to compare the actual dose delivered during in-vivo intravascular brachytherapy with the target range determined from the patient's prescribed dose. Furthermore, differences in dose distribution between a simplified tubular model (STM) and a geometrically correct 3-D model (GCM) obtained from fusion between biplane angiography and intravascular ultrasound were quantified. The tissue enclosed by the segmented lumen/plaque and media/adventitia borders was simulated using a structured finite-element mesh. The beta-radiation sources were modeled as 3-D objects in their angiographically determined locations. The accumulated dose was estimated using a fixed distance function based on the patient-specific radiation parameters. For visualization, the data was converted to VRML with the accumulated doses represented by color encoding. The statistical comparison between STM and GCM models in 8 patients showed that the STM significantly underestimates the dose delivered and its variability. The analysis revealed substantial deviations from the target dose range in curved vessels.

Keywords: Intravascular brachytherapy, intravascular ultrasound, X-ray angiography, 3-D multimodality fusion, image-guided procedures, beta radiation, coronary arteries, in-stent restenosis

1. INTRODUCTION

Coronary atherosclerosis is a common disease,[1] treatment of which gains increasing importance. Local obstructions (stenoses) in the arteries are usually treated by balloon angioplasty (PTCA) and stenting. As illustrated in Fig. 1, new plaque frequently accumulates at stented stenotic lesions, thus resulting in an in-stent restenosis.[2] To reduce the risk of re-occurrence of such restenosis following PTCA in the stented vessel segment, the lesion is treated afterwards with beta (β) or gamma (γ) radiation (intravascular brachytherapy).[3–7] The radiation is delivered by a "train" of sources that can be transported within a catheter into the vessel to be treated and remains there for a specified time before the train is retracted. For β-radiation, this application time is determined from the source activity and the angiographically estimated vessel diameter. Conventionally, a simplified model is used, assuming a straight vessel with the catheter centered and a constant-diameter circular cross section. However, vessel shape, curvature, and catheter location have a substantial impact on the actual dose delivered,[8] but are not considered in the current radiation models. The aim of this study was therefore to determine the actual dose delivered during in-vivo intravascular brachytherapy and to quantify the differences in dose distribution between a simplified tubular model and a geometrically correct three-dimensional (3-D) model derived from fusion between biplane angiography and intravascular ultrasound (IVUS). Figure 2 shows the appearance of in-stent restenosis in an in-vivo IVUS example. Our dosing model used for the simulations was adapted from

E-mail: <andreas-wahle@uiowa.edu>; http://www.engineering.uiowa.edu/~awahle; Fax: +1-319-335-6028

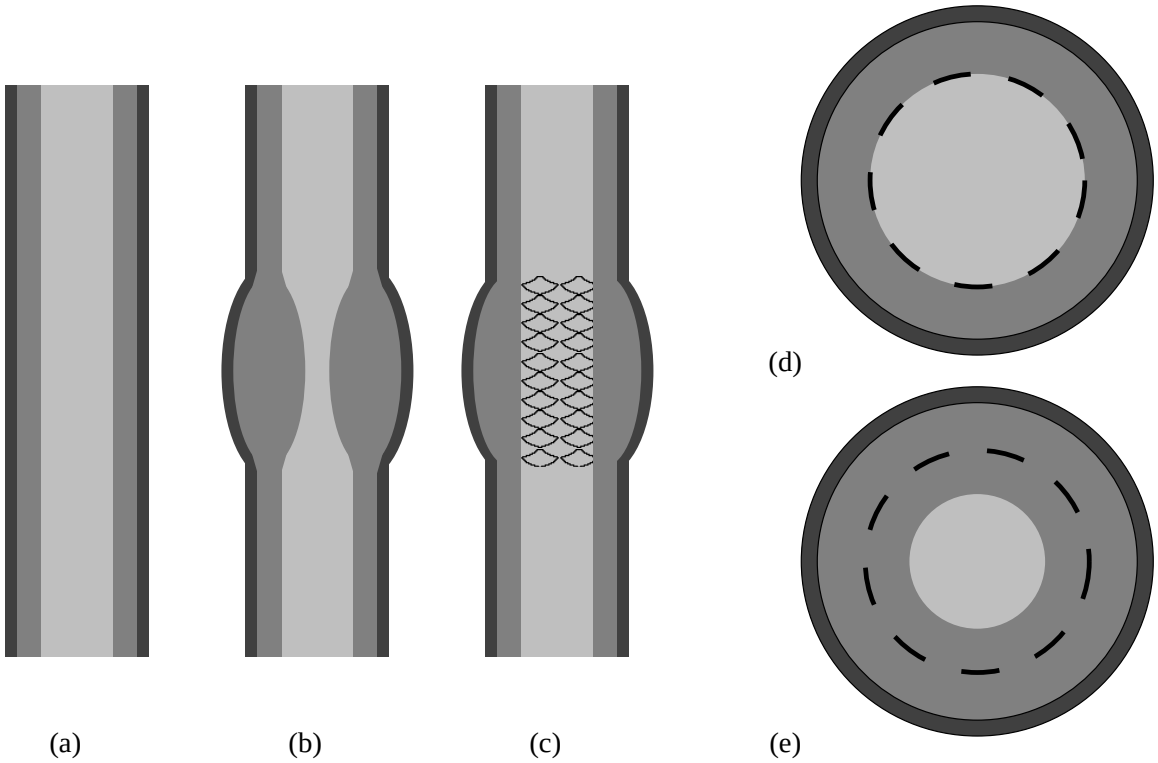

Figure 1. In-stent restenosis: (a) healthy vessel with media (dark), intimal layer with slight diffuse plaque (gray), and lumen (light gray); (b) stenosis with typical outward remodelling; (c) treated vessel segment, the lumen has been restored and a stent placed; (d) cross-sectional view with stent struts; (e) cross-sectional view after in-stent restenosis has developed.

experimental studies performed by Soares *et al.*[9,10] It has to be kept in mind however that dose prescription is still not well defined,[7] and that experimental gold standards which would provide the physically determined true doses for validation yet have to be established. Therefore, this study mainly focuses on determination of the relative impact of vessel curvature and catheter eccentricity on the dose delivered.

2. METHODS

To generate the geometrically correct model of the irradiated vessel segment, a well-established fusion system was used.[11–13] Our system utilizes biplane angiography to extract the vessel geometry as well as IVUS to obtain cross-sectional information. The IVUS transducer is placed well distally of the treated area, its location imaged with biplane angiography, and then pulled back using an automated pullback device. Filled with diluted contrast dye, the vessel lumen outline is also depicted in the angiograms and serves as a reference for the 3-D matching of the orientation of the IVUS frames (Fig. 3). The resulting data is sorted by heart phase according to the ECG signal,[13] segmented for lumen/plaque and media/adventitia borders, and then mapped into 3-D space based upon the angiographically determined pullback trajectory.[11,12] The tissue enclosed by the segmented lumen/plaque and media/adventitia borders is then modeled as a structured finite-element mesh with 4 layers and 72 radial segments per IVUS frame (Fig. 4). The location of the brachytherapy catheter is estimated relative to the stented segment from angiographic images. The simplified tubular model used for comparison was derived from the 3-D geometrically correct model by straightening, centering of the catheter, and reshaping each contour to co-axial circles with the same per-frame mean diameters as determined from the original data.[14]

Simulation of the intravascular brachytherapy procedure with ^{90}Sr/Y isotopes was performed by modeling the 12–16 β-radiation sources as line objects in 3-D. Each source consists of a 2.5 mm long element, 2.3 mm of which are considered the active length. The dose accumulating at any given point of the vessel was estimated

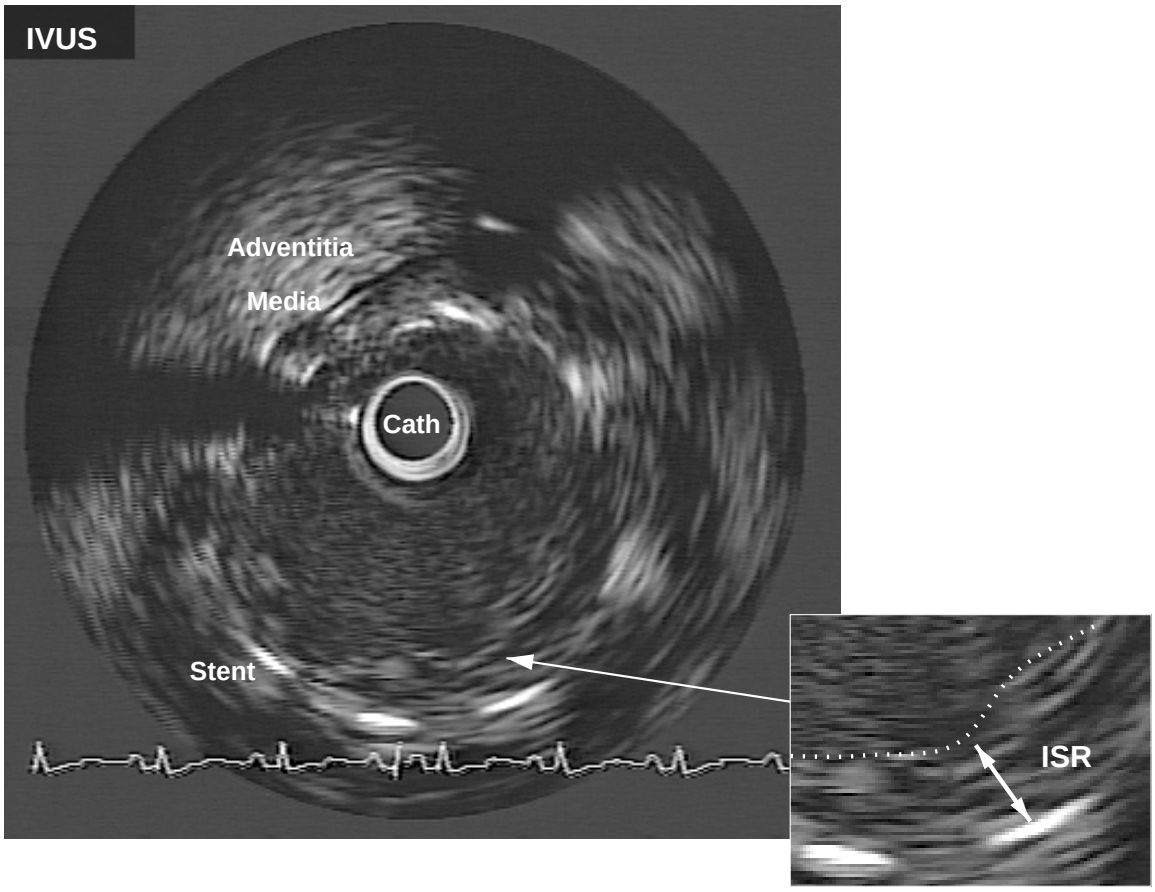

Figure 2. Example of in-stent (ISR) restenosis as visualized with in-vivo intravascular ultrasound; while the media is clearly visible in the upper-left corner as a dark band, it is less well visible behind the stent struts due to the compression of plaque during PTCA; blood speckle may make it difficult to differentiate between lumen and plaque (inset).

by using a fixed distance function based on previously published experimental data and the actually applied radiation parameters. In brief, the β-radiation received at any given point of the tissue is the sum D_p of the doses it received from all sources i of the radiation train:

$$D_i(r_{pi}) = \frac{C \cdot A_i \cdot t \cdot g(r_{pi})}{{r_{pi}}^2}$$

$$D_p = \sum_i D_i(r_{pi})$$

where C is a dose rate constant specific for the brachytherapy device; A_i is the activity of the source in giga-Becquerels (GBq), with usually the same A_i for all i within a train; t is the application time in seconds; and $g(r)$ is a polynomial-based radial dose function.[9, 14] Figure 5 shows the dose distribution for a typical dose prescription.

In addition to the simulation on in-vivo patient data, computer-generated phantoms were used to quantify the impact of vessel curvature and catheter eccentricity analytically.[14] In brief, the computer phantom used for testing was a 50 mm tube with nine coaxial layers between 1.0 and 5.0 mm radius in 0.5 mm intervals. It was represented as a structured finite-element mesh with a longitudinal resolution of 10 μm and a 1° width of the radial segments. To simulate vessel curvature, the tube could be "bent" by mapping it onto a torus segment

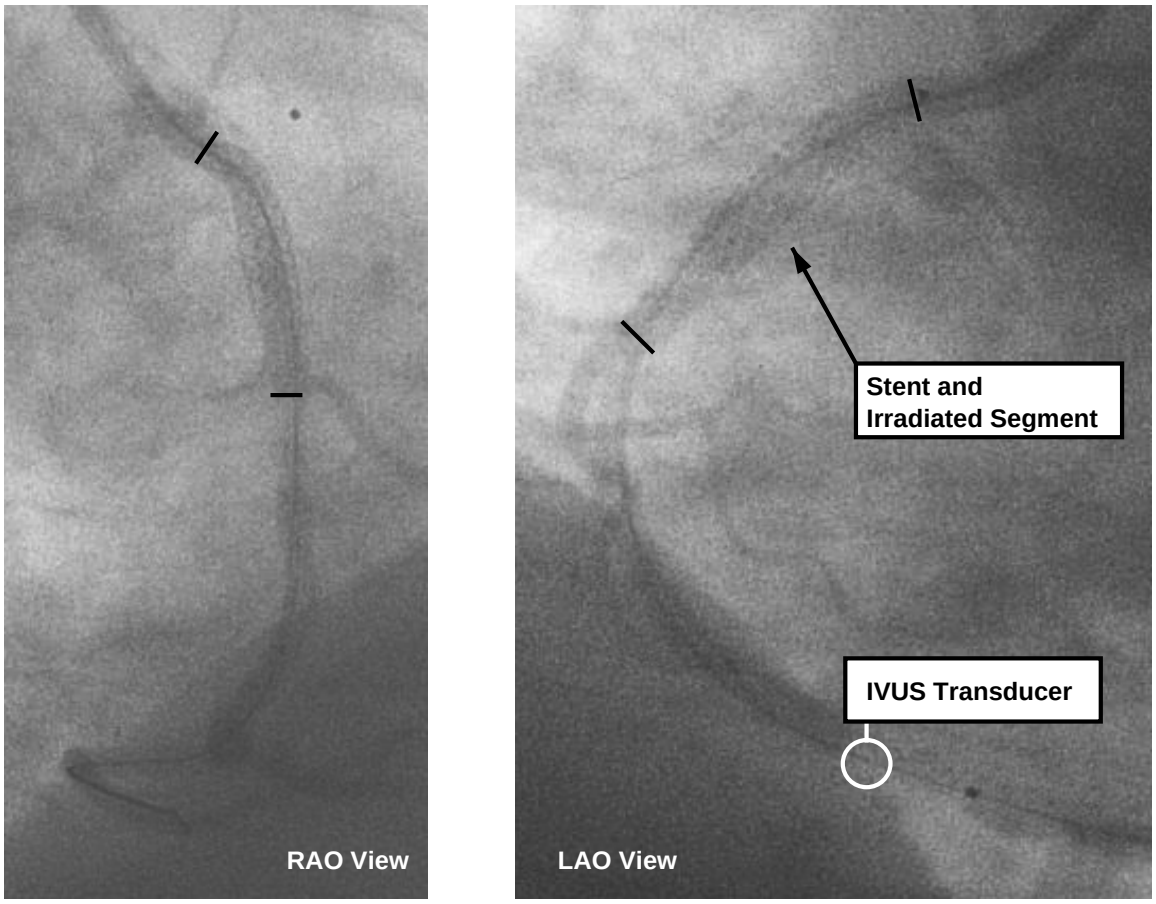

Figure 3. Biplane X-ray angiograms showing the irradiated vessel segment, the vessel lumen outline using diluted contrast dye, and the IVUS catheter within the lumen.

with an enclosed angle of up to 180° (Fig. 6). The eccentricity of the catheter was simulated by either linear offset or the superposition of a cosine waveform within that torus segment.

For each grid node, i.e., each intersection of the grid lines as shown in Fig. 4, the dose $D_p(f, l, s)$ received from all of the sources i was determined using above equations, where f is the frame number, l the layer number, and s specifies the radial segment. The respective doses were annotated to each of the nodes of the finite-element mesh. Other parameters, such as plaque thickness and local curvature,[15] are determined as well and added to the model in the same way. The finite-element meshes along with the simulation results were modeled in Tecplot* format. For quantitative analysis, the Tecplot data were converted for import into spreadsheet applications. For platform-independent 3-D visualization, the data was split into layers, triangulated, and converted to VRML[16] with the accumulated doses represented by color encoding (Fig. 7). The statistical analysis included the calculation of the mean dose and its standard deviation for all elements in the four individual layers of either geometrically correct or simplified tubular models. Furthermore, the percentages of elements receiving the target range defined by a patient-specific prescribed dose, as well as underdosing below and overdosing above certain thresholds were calculated.

3. RESULTS

The current set of individuals includes 11 patients subjected to intravascular brachytherapy, 8 of which were evaluated thus far in this ongoing study. Two patients had adjacent irradiations in the same vessel to cover a

*Tecplot is a registered trademark of Amtec Engineering Inc., Bellevue, WA 98009, USA

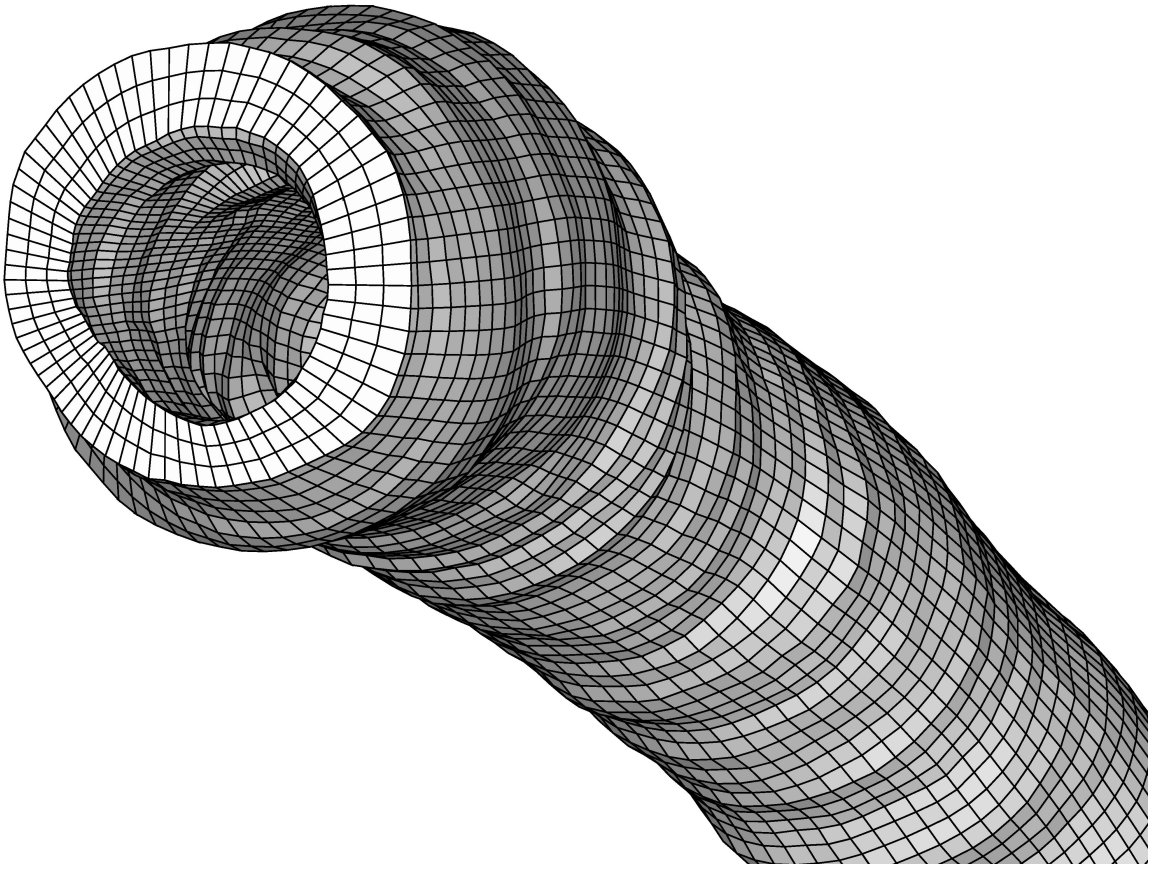

Figure 4. Reconstructed 3-D model of the vessel seen in Figs. 2–3, showing the grid structure with four layers and 72 radial segments; the longitudinal resolution is a factor of pullback speed and heart rate.

larger segment, thus the following data are based on a total of 10 irradiated vessel segments. The prescribed doses ranged from 18.4 to 25.3 Gy in 2 mm distance from the radiation catheter. The target range describes the desired range of doses within the entire vessel wall rather than in a single distance layer and was defined as a dose window of ±5 Gy centered at the prescribed dose. Between 20,160 and 61,920 grid points were generated per vessel, where (depending on train length and longitudinal grid resolution) from 15,264 to 29,664 grid points were located within the boundaries of the radiation source trains. As simulated, the target range of doses was delivered for 46.1% of the media/adventitia elements within the train boundaries over all 10 vessel segments; underdosing (<10 Gy) occurred in 0.8% at the lumen/plaque and 14.0% at the media/adventitia borders; overdosing (>30 Gy) was found in 6.3% of the media/adventitia elements. Within the set of patients, between 16.9 and 68.7% of media/adventitia elements satisfied their individual target range, thus indicating a high variability between subjects. In comparison of the simplified tubular (STM) vs. the geometrically correct model (GCM), the STM suggested significantly and systematically lower doses within the train boundaries ($p<0.001$). The average underestimation of dose of the STM relative to the GCM within the four layers was 3.04 Gy (lumen/plaque) to 1.13 Gy (media/adventitia). By ignoring vessel contour and catheter location, the STM also estimates a significantly lower level of dose variability than estimated from the GCM ($p<0.001$). The tubular STM predicted standard deviations of dose from 5.11 Gy at the lumen/plaque interface to 3.71 Gy at the media/adventitia interface, thus substantially lower than the dose variation of 11.93 Gy and 6.72 Gy, respectively, as assessed by the geometrically correct GCM.

The simulations on the computer-generated phantoms supported the hypothesis that vessel curvature and catheter eccentricity influence dose distribution. The torus experiments (Fig. 6) revealed that the dose increases towards the inner curvature and decreases towards the outer curvature with stronger bending of the tube: at 60° curvature, inside doses were increased by 2.95% and outside doses were decreased by 2.70%; a 180° torus segment

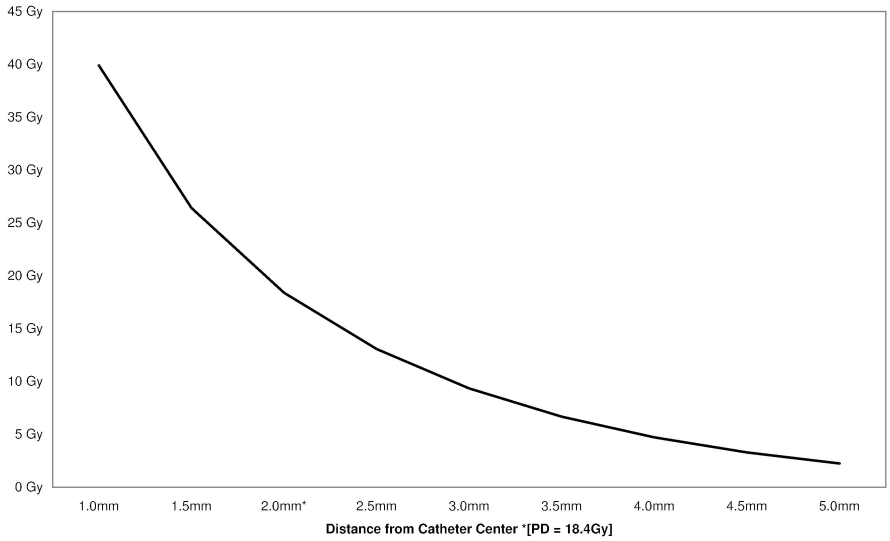

Figure 5. Fall-off curve for in the center of the brachytherapy train, simulated in layers of 0.5 mm intervals; dosing parameters included $C = 0.0164\,\mathrm{Gy/GBqs}$, $A_i = 0.136\,\mathrm{GBq}$, and $t = 180\,\mathrm{s}$.

showed an inside increase of 9.70% with an outside decrease of 7.48% relative to the straight tube. Catheter eccentricity has an even larger impact: with a simulated 18.389 Gy in 2 mm distance, shifting the source train by 0.5 mm towards that point increased radiation to 26.405 Gy, shifting the train 0.5 mm away from that point decreased radiation to 13.069 Gy. The values are approximately double and halve, respectively, of the original dose for an offset of 1.0 mm in either direction.

4. DISCUSSION

The presented study performing computer simulations on in-vivo data and on computer-generated phantoms demonstrated that vessel curvature and eccentricity of the delivery catheter have a substantial impact on the dose distribution. Common assumptions made in conventional dose-delivery models are likely to introduce systematic and significant errors. As illustrated in Fig. 7, the dose distribution is biased towards higher doses at the outer curvature of a strongly curved vessel like the right coronary artery, since the delivery catheter is forced against the vessel wall. A more homogeneous distribution, but still with very high local variances, can be seen in straighter vessels.

While it has to be kept in mind that the estimated absolute dose values yet remain unvalidated, and the dose model can and will be improved in the future, the tendencies derived from this study are already obvious. For example, the underestimation of dose variability by the STM as compared to the GCM will remain valid regardless of the absolute values. Another problem is that the overall processing pipeline of data acquisition, segmentation, and analysis is time-consuming and needs manual supervision. Especially, the segmentation of the IVUS data is a challenging task due to ambiguities, calcific shadowing, and compressed plaque (Fig. 2).[17, 18] Further research will also be performed towards the differentiation between plaque types, which then can be used in a more sophisticated dosing model, e.g., based on Monte-Carlo simulations.[19, 20]

5. CONCLUSIONS

In conclusion, dose-assessment models for intravascular brachytherapy that do not consider factors like the location of the radiation catheter within the vessel as well as the shape and curvature of the vessel result in significant underestimation of dose variability and the radiation delivered as compared to a geometrically correct model. We have developed a method to estimate the actual dose delivered to each point of the treated vessel segment, as accurately reconstructed by fusion from biplane angiography and intravascular ultrasound, thus allowing to identify possible locations of over- or underdosing in the actual geometry of the patient's vessel.

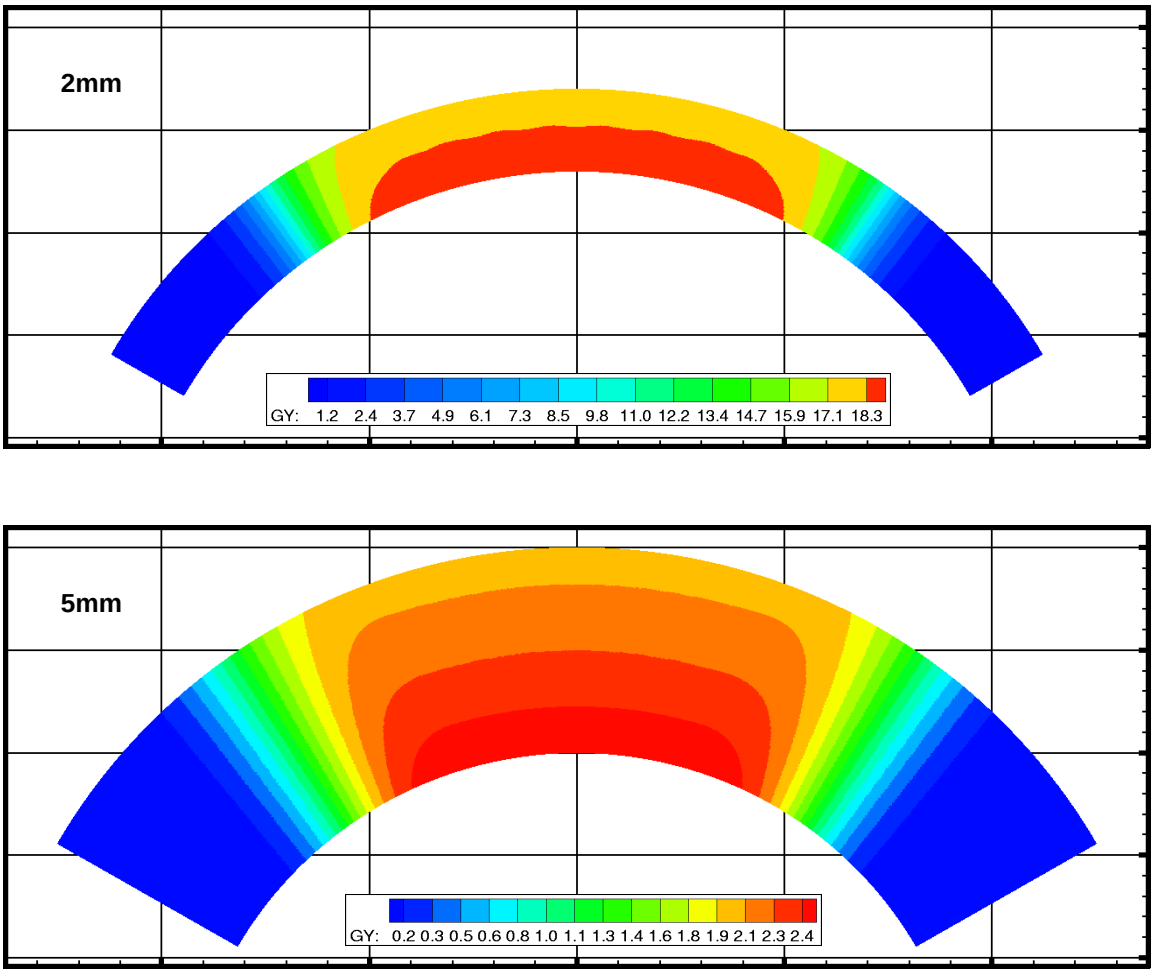

Figure 6. Simulation results on a 120°-torus (50 mm arc length with a 30 mm 12-source centered radiation train) with a prescribed dose of 18.4 Gy at 2 mm distance; the increase of dose towards the inner curvature is clearly demonstrated *(this figure is available in color on the CD version or the authors' web page).*

ACKNOWLEDGMENTS

This work was supported in part by grant R01 HL63373 of the Heart, Lung, and Blood Institute at NIH, Bethesda, MD 20892, USA. The authors would like to thank Steven C. Mitchell and Mark E. Olszewski, graduate students in Electrical and Computer Engineering at The University of Iowa, for their contributions to the development of the image data fusion system for geometrically correct reconstruction of coronary arteries in vivo.

REFERENCES

1. American Heart Association, *2001 Heart and Stroke Statistical Update*, AHA, Dallas, 2000.
2. G. S. Mintz, J. J. Popma, A. D. Pichard, K. M. Kent, L. F. Satler, S. C. Wong, M. K. Hong, J. A. Kovach, and M. B. Leon, "Arterial remodeling after coronary angioplasty: A serial intravascular ultrasound study," *Circulation* **94**, pp. 35–43, July 1996.
3. R. Waksman, B. Bhargava, J. F. Saucedo, R. C. Chan, F. O. Tio, Y. Vodovotz, and V. Verin, "Yttrium-90 delivered via a centering catheter and afterloader, given both before and after stent implantation, inhibits neointima formation in porcine coronary arteries," *Cardiovascular Radiation Medicine* **2**, pp. 11–17, Jan.-Mar. 2000.

4. R. E. Kuntz and D. S. Baim, "Prevention of coronary restenosis: The evolving evidence base for radiation therapy," *Circulation* **101**, pp. 2130–2133, May 2000.
5. M. Sabaté, J. P. A. Marijnissen, S. G. Carlier, I. P. Kay, W. J. van der Giessen, V. L. M. A. Coen, J. M. R. Ligthart, E. Boersma, M. A. Costa, P. C. Levendag, and P. W. Serruys, "Residual plaque burden, delivered dose, and tissue composition predict 6-month outcome after balloon angioplasty and beta-radiation therapy," *Circulation* **101**, pp. 2472–2477, May 2000.
6. G. S. Mintz, N. J. Weissman, and P. J. Fitzgerald, "Intravascular ultrasound assessment of the mechanisms and results of brachytherapy," *Circulation* **104**, pp. 1320–1325, Sept. 2001.
7. R. A. Fox, "Intravascular brachytherapy of the coronary arteries," *Physics in Medicine and Biology* **47**, pp. R1–R30, Feb. 2002.
8. S. G. Carlier, J. P. A. Marijnissen, V. L. M. A. Coen, W. J. van der Giessen, M. Sabaté, J. M. R. Ligthart, A. den Boer, I. E. Céspedes, W. Li, A. F. W. van der Steen, P. C. Levendag, and P. W. Serruys, "Guidance of intracoronary radiation therapy based on dose-volume histograms derived from quantitative intravascular ultrasound," *IEEE Transactions on Medical Imaging* **17**, pp. 772–778, Oct. 1998.
9. C. G. Soares, D. G. Halpern, and C. K. Wang, "Calibration and characterization of beta-particle sources for intravascular brachytherapy," *Medical Physics* **25**, pp. 339–346, Mar. 1998.
10. R. Nath, H. I. Amols, C. W. Coffey, D. M. Duggan, S. K. Jani, Z. Li, M. C. Schell, C. G. Soares, J. S. Whiting, P. E. Cole, I. R. Crocker, and R. S. Schwartz, "Intravascular brachytherapy physics: Report of the AAPM radiation therapy committee task group #60," *Medical Physics* **26**, pp. 119–152, Feb. 1999.
11. A. Wahle, G. P. M. Prause, S. C. DeJong, and M. Sonka, "Geometrically correct 3-D reconstruction of intravascular ultrasound images by fusion with biplane angiography — methods and validation," *IEEE Transactions on Medical Imaging* **18**, pp. 686–699, Aug. 1999.
12. A. Wahle, G. P. M. Prause, C. von Birgelen, R. Erbel, and M. Sonka, "Fusion of angiography and intravascular ultrasound in-vivo: Establishing the absolute 3-D frame orientation," *IEEE Transactions on Biomedical Engineering — Biomedical Data Fusion* **46**, pp. 1176–1180, Oct. 1999.
13. A. Wahle, S. C. Mitchell, S. D. Ramaswamy, K. B. Chandran, and M. Sonka, "Four-dimensional coronary morphology and computational hemodynamics," in *Medical Imaging 2001: Image Processing*, M. Sonka and K. M. Hanson, eds., **4322**, pp. 743–754, SPIE Proceedings, (Bellingham WA), 2001.
14. A. Wahle, J. J. Lopez, E. C. Pennington, S. L. Meeks, K. C. Braddy, J. M. Fox, T. M. H. Brennan, J. M. Buatti, J. D. Rossen, and M. Sonka, "Effects of vessel geometry and catheter position on dose delivery in intracoronary brachytherapy," *IEEE Transactions on Biomedical Engineering* **50**, expected 2003. (submitted and revised).
15. A. Wahle, R. Medina, K. C. Braddy, J. M. Fox, T. M. H. Brennan, J. J. Lopez, J. D. Rossen, and M. Sonka, "Impact of local vessel curvature on the circumferential plaque distribution in coronary arteries," in *Medical Imaging 2003: Physiology and Function: Methods, Systems, and Applications*, A. V. Clough and A. A. Amini, eds., **5031**, SPIE Proceedings, (Bellingham WA), 2003.
16. ISO/IEC 14772, "Information technology — computer graphics and image processing — the virtual reality modeling language." International Organization for Standardization, Geneva CH, 1998.
17. X. Zhang, C. R. McKay, and M. Sonka, "Tissue characterization in intravascular ultrasound images," *IEEE Transactions on Medical Imaging* **17**, pp. 889–899, Dec. 1998.
18. P. M. Stähr, T. Höfflinghaus, T. Voigtländer, B. K. Courtney, A. Victor, M. Otto, P. G. Yock, R. Brennecke, and P. J. Fitzgerald, "Discrimination of early/intermediate and advanced/complicated coronary plaque types by radiofrequency intravascular ultrasound analysis," *American Journal of Cardiology* **90**, pp. 19–23, July 2002.
19. V. Sehgal, Z. Li, J. R. Palta, K. M. Smith, and W. E. Bolch, "Application of imaging-derived parameters to dosimetry of intravascular brachytherapy sources: Perturbation effects of residual plaque burden," *Medical Physics* **29**, pp. 1580–1589, July 2002.
20. R. Wang and X. A. Li, "Monte Carlo dose calculations of beta-emitting sources for intravascular brachytherapy: A comparison between EGS4, EGSnrc, and MCNP," *Medical Physics* **28**, pp. 134–141, Feb. 2001.

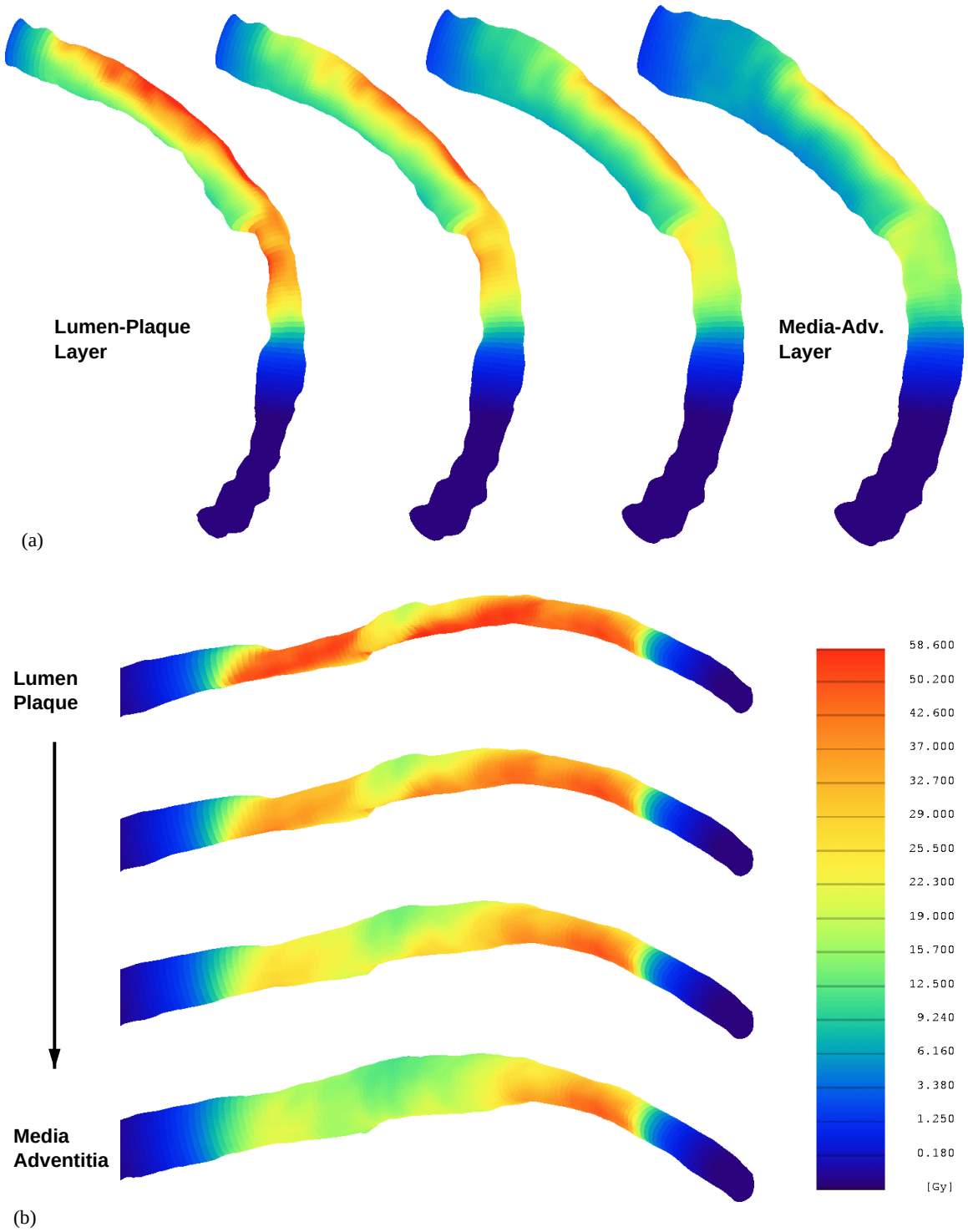

Figure 7. Calculated dose distribution visualized in VRML and split up into the four layers; (a) of the vessel shown in Figs. 2–4 with a strong curvature and eccentricity of the brachytherapy catheter; (b) a moderately curved vessel segment of an in-vivo left-anterior-descending artery *(this figure is available in color on the CD version or the authors' web page).*